
Supplementary information

A photonic quantum engine driven by superradiance

In the format provided by the authors and unedited

Supplementary Information for “A photonic quantum engine driven by superradiance”

Jinuk Kim,¹ Seunghoon Oh,¹ Daeho Yang,² Junki Kim,³ Moonjoo Lee,⁴ and Kyungwon An^{1, *}

¹*Department of Physics and Astronomy & Institute of Applied Physics, Seoul National University, Seoul 08826, Korea*

²*Samsung Advanced Institute of Technology, Samsung Electronics, Suwon 16678, Gyeonggi-do, Korea*

³*SKKU Advanced Institute of Nano Technology, Sungkyunkwan University, Suwon 16419, Korea*

⁴*Department of Electrical Engineering, Pohang University of Science and Technology(POSTECH), Pohang 37673, Korea*

1. THEORY OF THE SUPERRADIANT RESERVOIR

To describe a cavity coupled to an atomic beam reservoir, we derive a master equation from the single atom-cavity Jaynes-Cummings Hamiltonian. The Hamiltonian is given by

$$H_{\text{AF}}/\hbar = \frac{\Delta_{\text{ac}}}{2}\sigma_z + g(\sigma^\dagger a + \sigma a^\dagger), \quad (\text{S1})$$

where $\Delta_{\text{ac}} = \omega_a - \omega_c$ represents the atom-cavity detuning, σ_z denotes the inversion operator, g is the atom-cavity coupling constant and $\sigma^\dagger(\sigma)$ is the raising(lowering) operator of the atom and $a(a^\dagger)$ is the annihilation(creation) operator for photons. According to Ref. [1], the unitary evolution operator $U(\tau)$ can be written as

$$\begin{aligned} U(\tau) &= e^{-iH_{\text{AF}}\tau/\hbar} = \sum_{n=0}^{\infty} \frac{(-i\tau/\hbar)^n}{n!} H_{\text{AF}}^n \\ &= \begin{pmatrix} \cos(\Omega_n\tau/2) - i\Delta_{\text{ac}}\tau/2 \operatorname{sinc}(\Omega_n\tau/2) & -ig\tau \operatorname{sinc}(\Omega_n\tau/2)a \\ -ig\tau a^\dagger \operatorname{sinc}(\Omega_{n-1}\tau/2) & \cos(\Omega_{n-1}\tau/2) + i\Delta_{\text{ac}}\tau/2 \operatorname{sinc}(\Omega_{n-1}\tau/2) \end{pmatrix}, \end{aligned} \quad (\text{S2})$$

where $\Omega_n \equiv \sqrt{\Delta_{\text{ac}}^2 + 4g^2(a^\dagger a + 1)}$ and the representations $|e\rangle = \begin{pmatrix} 1 \\ 0 \end{pmatrix}$ and $|g\rangle = \begin{pmatrix} 0 \\ 1 \end{pmatrix}$ are used. If $\sqrt{n+1}g\tau \ll 1$, expanding to the second order of $g\tau$, we obtain

$$\begin{aligned} \cos(\Omega_n\tau/2) &\simeq \cos(\Delta_{\text{ac}}\tau/2) - \frac{1}{2} \operatorname{sinc}(\Delta_{\text{ac}}\tau/2) (g\tau)^2 (a^\dagger a + 1), \\ \operatorname{sinc}(\Omega_n\tau/2) &\simeq \operatorname{sinc}(\Delta_{\text{ac}}\tau/2) + \frac{2}{(\Delta_{\text{ac}}\tau)^2} \{\cos(\Delta_{\text{ac}}\tau/2) - \operatorname{sinc}(\Delta_{\text{ac}}\tau/2)\} (g\tau)^2 (a^\dagger a + 1). \end{aligned} \quad (\text{S3})$$

After the interaction time τ , the atom leaves the cavity. The state of the cavity can be calculated by tracing out the atom, $\rho(\tau) = \operatorname{Tr}_a [U(\tau)\rho_{\text{AF}}(0)U(\tau)^\dagger] = \langle g|U(\tau)\rho_{\text{AF}}(0)U(\tau)^\dagger|g\rangle + \langle e|U(\tau)\rho_{\text{AF}}(0)U(\tau)^\dagger|e\rangle$, where $\rho(t)(\rho_{\text{AF}}(t))$ is the cavity field(atom-field) density matrix. With foregoing approximations, we obtain

$$\begin{aligned} \langle g|U(\tau) &= \left\{ -\frac{1}{2} \operatorname{sinc}(\Delta_{\text{ac}}\tau/2) + \frac{i}{\Delta_{\text{ac}}\tau} (\cos(\Delta_{\text{ac}}\tau/2) - \operatorname{sinc}(\Delta_{\text{ac}}\tau/2)) \right\} (g\tau)^2 a^\dagger a \langle g| \\ &\quad + e^{i\Delta_{\text{ac}}\tau/2} \langle g| - ig\tau \operatorname{sinc}(\Delta_{\text{ac}}\tau/2) a^\dagger \langle e|, \\ \langle e|U(\tau) &= \left\{ -\frac{1}{2} \operatorname{sinc}(\Delta_{\text{ac}}\tau/2) - \frac{i}{\Delta_{\text{ac}}\tau} (\cos(\Delta_{\text{ac}}\tau/2) - \operatorname{sinc}(\Delta_{\text{ac}}\tau/2)) \right\} (g\tau)^2 a a^\dagger \langle e| \\ &\quad + e^{-i\Delta_{\text{ac}}\tau/2} \langle e| - ig\tau \operatorname{sinc}(\Delta_{\text{ac}}\tau/2) a \langle g|. \end{aligned} \quad (\text{S4})$$

This yields

$$\begin{aligned}
\rho(\tau) = & \rho(0) + \rho_{ee} (g\tau \operatorname{sinc}(\Delta_{ac}\tau/2))^2 a^\dagger \rho(0) a - ig\tau \operatorname{sinc}(\Delta_{ac}\tau/2) \rho_{eg} a^\dagger \rho(0) e^{-i\Delta_{ac}\tau/2} \\
& + \rho_{gg} (g\tau \operatorname{sinc}(\Delta_{ac}\tau/2))^2 a \rho(0) a^\dagger - ig\tau \operatorname{sinc}(\Delta_{ac}\tau/2) \rho_{ge} a \rho(0) e^{i\Delta_{ac}\tau/2} \\
& + ig\tau \operatorname{sinc}(\Delta_{ac}\tau/2) \rho_{eg} \rho(0) a^\dagger e^{-i\Delta_{ac}\tau/2} + ig\tau \operatorname{sinc}(\Delta_{ac}\tau/2) \rho_{ge} \rho(0) a e^{i\Delta_{ac}\tau/2} \\
& + \rho_{gg} e^{-i\Delta_{ac}\tau/2} \left\{ -\frac{1}{2} \operatorname{sinc}(\Delta_{ac}\tau/2) + \frac{i}{\Delta_{ac}\tau} (\cos(\Delta_{ac}\tau/2) - \operatorname{sinc}(\Delta_{ac}\tau/2)) \right\} (g\tau)^2 a^\dagger a \rho(0) \\
& + \rho_{gg} e^{i\Delta_{ac}\tau/2} \left\{ -\frac{1}{2} \operatorname{sinc}(\Delta_{ac}\tau/2) - \frac{i}{\Delta_{ac}\tau} (\cos(\Delta_{ac}\tau/2) - \operatorname{sinc}(\Delta_{ac}\tau/2)) \right\} (g\tau)^2 \rho(0) a^\dagger a \\
& + \rho_{ee} e^{i\Delta_{ac}\tau/2} \left\{ -\frac{1}{2} \operatorname{sinc}(\Delta_{ac}\tau/2) - \frac{i}{\Delta_{ac}\tau} (\cos(\Delta_{ac}\tau/2) - \operatorname{sinc}(\Delta_{ac}\tau/2)) \right\} (g\tau)^2 a a^\dagger \rho(0) \\
& + \rho_{ee} e^{-i\Delta_{ac}\tau/2} \left\{ -\frac{1}{2} \operatorname{sinc}(\Delta_{ac}\tau/2) + \frac{i}{\Delta_{ac}\tau} (\cos(\Delta_{ac}\tau/2) - \operatorname{sinc}(\Delta_{ac}\tau/2)) \right\} (g\tau)^2 \rho(0) a a^\dagger \\
& + \mathcal{O}\left((g\tau)^3\right),
\end{aligned} \tag{S5}$$

where ρ_{ee} and ρ_{gg} (ρ_{eg} and ρ_{ge}) denote (off-)diagonal elements of the density matrix of the injected atom. Using the Lindblad operator defined as $\mathcal{L}[a]\rho = a\rho a^\dagger - \frac{1}{2}(a^\dagger a\rho + \rho a^\dagger a)$ and defining a new function $f(\Delta_{ac})$, Eq. (S5) can be simplified to

$$\begin{aligned}
\rho(\tau) - \rho(0) = & (g\tau \operatorname{sinc}(\Delta_{ac}\tau/2))^2 \rho_{ee} \mathcal{L}[a^\dagger] \rho(0) + (g\tau \operatorname{sinc}(\Delta_{ac}\tau/2))^2 \rho_{gg} \mathcal{L}[a] \rho(0) \\
& + i\rho_{gg} f(\Delta_{ac}) (g\tau)^2 a^\dagger a \rho(0) - i\rho_{gg} f(\Delta_{ac}) (g\tau)^2 \rho(0) a^\dagger a \\
& - i\rho_{ee} f(\Delta_{ac}) (g\tau)^2 a a^\dagger \rho(0) + i\rho_{ee} f(\Delta_{ac}) (g\tau)^2 \rho(0) a a^\dagger \\
& + ig\tau \operatorname{sinc}(\Delta_{ac}\tau/2) \left\{ -\rho_{eg} a^\dagger \rho(0) e^{-i\Delta_{ac}\tau/2} - \rho_{ge} a \rho(0) e^{i\Delta_{ac}\tau/2} \right\} \\
& + ig\tau \operatorname{sinc}(\Delta_{ac}\tau/2) \left\{ \rho_{ge} \rho(0) a e^{i\Delta_{ac}\tau/2} + \rho_{eg} \rho(0) a^\dagger e^{-i\Delta_{ac}\tau/2} \right\} \\
& + \mathcal{O}\left((g\tau)^3\right),
\end{aligned} \tag{S6}$$

where

$$f(\Delta_{ac}) \equiv \frac{\cos(\Delta_{ac}\tau/2)}{\Delta_{ac}\tau} \{ \cos(\Delta_{ac}\tau/2) - \operatorname{sinc}(\Delta_{ac}\tau/2) \} + \frac{1}{2} \sin(\Delta_{ac}\tau/2) \operatorname{sinc}(\Delta_{ac}\tau/2). \tag{S7}$$

If τ is shorter than the characteristic time of field growth or decay, the time derivative of density matrix can be approximated as $\dot{\rho}(t) \simeq \frac{\rho(\tau) - \rho(0)}{\tau}$. This gives

$$\dot{\rho}(t) = -\frac{i}{\hbar} [H, \rho(t)] + \frac{N}{\tau} (g\tau \operatorname{sinc}(\Delta_{ac}\tau/2))^2 \rho_{ee} \mathcal{L}[a^\dagger] \rho(t) + \frac{N}{\tau} (g\tau \operatorname{sinc}(\Delta_{ac}\tau/2))^2 \rho_{gg} \mathcal{L}[a] \rho(t), \tag{S8}$$

where each term has been multiplied by the average number \bar{N} of atoms in the cavity to account for multiple atoms. More rigorous extension for many atoms can be found in Refs. [2, 3]. The Hamiltonian H can be written as

$$H/\hbar \equiv -\gamma_{\text{inj}} (\rho_{gg} - \rho_{ee}) f(\Delta_{ac}) (g\tau)^2 a^\dagger a + \gamma_{\text{inj}} g\tau \operatorname{sinc}(\Delta_{ac}\tau) \left(\rho_{eg} a^\dagger e^{-i\Delta_{ac}\tau/2} + \rho_{ge} a e^{i\Delta_{ac}\tau/2} \right), \tag{S9}$$

where $\gamma_{\text{inj}} \equiv \bar{N}/\tau$ denotes the atomic injection rate. The first term represents frequency pulling/pushing effect, which is negligible for the experimental parameters in the manuscript. In Eq. (S8), the second(third) term corresponds to the upper(lower) energy level of the atomic reservoir. The ratio of the coefficients in front of the Lindblad operators can be equated to the Boltzmann factor to define the temperature of the atomic reservoir.

$$\frac{\rho_{ee}}{\rho_{gg}} = \exp\left(-\frac{\hbar\omega_a}{k_B T_{\text{atom}}}\right) \tag{S10}$$

We now include the cavity decay by adding $2\kappa\mathcal{L}[a]\rho(t)$ to the righthand side of Eq. (S8). The result can be rearranged as follows:

$$\dot{\rho}(t) = -\frac{i}{\hbar} [H, \rho(t)] + \Gamma_r \bar{n}_{\text{th}} \mathcal{L}[a^\dagger] \rho(t) + \Gamma_r (\bar{n}_{\text{th}} + 1) \mathcal{L}[a] \rho(t), \tag{S11}$$

where the thermal photon number and decay constant are defined as $\bar{n}_{\text{th}} \equiv \frac{\rho_{\text{ee}}\gamma_{\text{inj}}\{g\tau \text{sinc}(\Delta_{\text{ac}}\tau/2)\}^2}{(\rho_{\text{gg}} - \rho_{\text{ee}})\gamma_{\text{inj}}\{g\tau \text{sinc}(\Delta_{\text{ac}}\tau/2)\}^2 + 2\kappa}$, and $\Gamma_{\text{r}} \equiv (\rho_{\text{gg}} - \rho_{\text{ee}})\gamma_{\text{inj}}\{g\tau \text{sinc}(\Delta_{\text{ac}}\tau/2)\}^2 + 2\kappa$, respectively. In the presence of the cavity decay, the second(third) term in Eq. (S11) corresponds to the upper(lower) energy level of a redefined reservoir composed of atoms and the photonic vacuum associated with the cavity decay. The temperature of the new reservoir is given by

$$\frac{\bar{n}_{\text{th}}}{\bar{n}_{\text{th}} + 1} = \exp\left(-\frac{\hbar\omega_{\text{a}}}{k_{\text{B}}T_{\text{R}}}\right), \quad (\text{S12})$$

which has the same form as the one describing a thermal reservoir containing \bar{n}_{th} photons.

Eqs. (S11) and (S12) show that atoms and a photonic vacuum form a single heat reservoir of temperature T_{R} and this is the heat reservoir that is employed in our experiment. It might be more rigorous to describe the engine as being driven by many baths. However, in our experiment, photonic vacuum is an irremovable element and it does not play an important role in driving the quantum engine: it has no quantum coherence and thus does not provide energy to the working fluid. Therefore, it is more practical to incorporate it into a single heat reservoir characterized by a single temperature as in Eqs. (S11) and (S12).

2. STEADY STATE : THERMAL COHERENT STATE

The steady state solution ρ_{ss} satisfies

$$0 = -\frac{i}{\hbar}[H, \rho_{\text{ss}}] + \Gamma_{\text{r}}\bar{n}_{\text{th}}\mathcal{L}[a^\dagger]\rho_{\text{ss}} + \Gamma_{\text{r}}(\bar{n}_{\text{th}} + 1)\mathcal{L}[a]\rho_{\text{ss}}. \quad (\text{S13})$$

We introduce a thermal coherent state $\rho_{\text{ss}} = D(\alpha)\rho_{\text{th}}D^\dagger(\alpha)$ as an ansatz for solving the above equation, where $D(\alpha) \equiv e^{\alpha a^\dagger - \alpha^* a}$ is a displacement operator, and $\rho_{\text{th}} \equiv \sum_k \frac{\bar{n}_{\text{th}}^k}{(1 + \bar{n}_{\text{th}})^{k+1}} |k\rangle \langle k|$. Here, α is an arbitrary complex number. Let us apply $D^\dagger(\alpha)$ on the left and $D(\alpha)$ on the right. Using the relations $D(\alpha)^\dagger a D(\alpha) = a + \alpha$, and $D(\alpha)^\dagger a^\dagger D(\alpha) = a^\dagger + \alpha^*$, we find

$$\begin{aligned} D^\dagger(\alpha)\mathcal{L}[a]\rho_{\text{ss}}D(\alpha) &= (a + \alpha)\rho_{\text{th}}(a^\dagger + \alpha^*) - \frac{1}{2}\{(a^\dagger + \alpha^*)(a + \alpha)\rho_{\text{th}} + \rho_{\text{th}}(a^\dagger + \alpha^*)(a + \alpha)\} \\ &= \mathcal{L}[a]\rho_{\text{th}} + \frac{1}{2}\{(\alpha^* a - \alpha a^\dagger)\rho_{\text{th}} + \rho_{\text{th}}(\alpha a^\dagger - \alpha^* a)\}, \end{aligned} \quad (\text{S14})$$

$$\begin{aligned} D^\dagger(\alpha)\frac{i}{\hbar}[H, \rho_{\text{ss}}]D(\alpha) &= i\gamma_{\text{inj}}g\tau \text{sinc}(\Delta_{\text{ac}}\tau/2)D^\dagger(\alpha)\left(\rho_{\text{eg}}a^\dagger e^{-i\Delta_{\text{ac}}\tau/2} + \rho_{\text{ge}}a e^{i\Delta_{\text{ac}}\tau/2}\right)D(\alpha)\rho_{\text{th}} \\ &\quad - i\gamma_{\text{inj}}g\tau \text{sinc}(\Delta_{\text{ac}}\tau/2)\rho_{\text{th}}D^\dagger(\alpha)\left(\rho_{\text{eg}}a^\dagger e^{-i\Delta_{\text{ac}}\tau/2} + \rho_{\text{ge}}a e^{i\Delta_{\text{ac}}\tau/2}\right)D(\alpha) \\ &= -i\gamma_{\text{inj}}g\tau \text{sinc}(\Delta_{\text{ac}}\tau/2)\left[\rho_{\text{th}}, \rho_{\text{eg}}a^\dagger e^{-i\Delta_{\text{ac}}\tau/2} + \rho_{\text{ge}}a e^{i\Delta_{\text{ac}}\tau/2}\right]. \end{aligned} \quad (\text{S15})$$

Substitution of the above results into Eq. (S13) gives

$$\begin{aligned} &i\gamma_{\text{inj}}g\tau \text{sinc}(\Delta_{\text{ac}}\tau/2)\left[\rho_{\text{th}}, \rho_{\text{eg}}a^\dagger e^{-i\Delta_{\text{ac}}\tau/2} + \rho_{\text{ge}}a e^{i\Delta_{\text{ac}}\tau/2}\right] + \Gamma_{\text{r}}\bar{n}_{\text{th}}\mathcal{L}[a^\dagger]\rho_{\text{th}} + \Gamma_{\text{r}}(\bar{n}_{\text{th}} + 1)\mathcal{L}[a]\rho_{\text{th}} \\ &+ \frac{1}{2}\Gamma_{\text{r}}(\bar{n}_{\text{th}} + 1)\left[\rho_{\text{th}}, \alpha a^\dagger - \alpha^* a\right] + \frac{1}{2}\Gamma_{\text{r}}\bar{n}_{\text{th}}\left[\rho_{\text{th}}, \alpha^* a - \alpha a^\dagger\right] = 0. \end{aligned} \quad (\text{S16})$$

The sum of the second and the third terms vanishes, and the equation is simplified as

$$i\gamma_{\text{inj}}g\tau \text{sinc}(\Delta_{\text{ac}}\tau/2)\left[\rho_{\text{th}}, \rho_{\text{eg}}a^\dagger e^{-i\Delta_{\text{ac}}\tau/2} + \rho_{\text{ge}}a e^{i\Delta_{\text{ac}}\tau/2}\right] + \frac{1}{2}\Gamma_{\text{r}}\left[\rho_{\text{th}}, \alpha a^\dagger - \alpha^* a\right] = 0. \quad (\text{S17})$$

For the equation to hold, the value of α must be

$$\alpha = -2i\frac{\gamma_{\text{inj}}}{\Gamma_{\text{r}}}g\tau \text{sinc}(\Delta_{\text{ac}}\tau/2)\rho_{\text{eg}}e^{-i\Delta_{\text{ac}}\tau/2}. \quad (\text{S18})$$

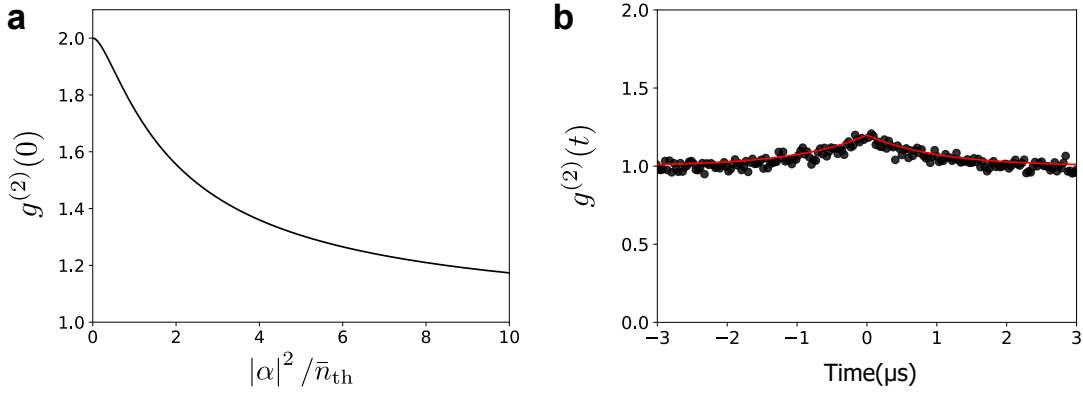


FIG. S1. **The second order correlation of the steady state** **a**, The photon number ratio dependence of the second-order correlation function at zero delay time. **b**, The second-order correlation measurement of the thermal coherent state. Black circles correspond experimental data and red solid curve is the analytic solution. Experiments were performed under the following condition: $N = 0.4$ and $gr = 0.03$.

The mean photon number and the second-order correlation function at zero delay time of the steady state can be calculated, respectively, as

$$\begin{aligned}
 \langle n \rangle &= \langle a^\dagger a \rho_{ss} \rangle = \bar{n}_{th} + |\alpha|^2, \tag{S19} \\
 g^{(2)}(0) &= \frac{\langle a^\dagger a^\dagger a a \rho_{ss} \rangle}{\langle a^\dagger a \rho_{ss} \rangle^2} = \frac{\langle a^\dagger a^\dagger a a D(\alpha) \rho_{th} D^\dagger(\alpha) \rangle}{(\bar{n}_{th} + |\alpha|^2)^2} \\
 &= \frac{\langle D^\dagger(\alpha) a^\dagger D(\alpha) D^\dagger(\alpha) a^\dagger D(\alpha) D^\dagger(\alpha) a D(\alpha) D^\dagger(\alpha) a D(\alpha) \rho_{th} \rangle}{(\bar{n}_{th} + |\alpha|^2)^2} \\
 &= \frac{\langle (a^\dagger + \alpha^*)^2 (a + \alpha)^2 \rho_{th} \rangle}{(\bar{n}_{th} + |\alpha|^2)^2} = \frac{\langle (a^{\dagger 2} a^2 + 4|\alpha|^2 a^\dagger a + |\alpha|^4) \rho_{th} \rangle}{(\bar{n}_{th} + |\alpha|^2)^2} \tag{S20} \\
 &= \frac{\langle a^{\dagger 2} a^2 \rho_{th} \rangle + 4|\alpha|^2 \bar{n}_{th} + |\alpha|^4}{(\bar{n}_{th} + |\alpha|^2)^2} = \frac{2\bar{n}_{th}^2 + 4|\alpha|^2 \bar{n}_{th} + |\alpha|^4}{(\bar{n}_{th} + |\alpha|^2)^2} \\
 &= 1 + \frac{1 + 2|\alpha|^2 / \bar{n}_{th}}{(1 + |\alpha|^2 / \bar{n}_{th})^2}.
 \end{aligned}$$

The second-order correlation function at zero delay time approaches unity as the ratio $|\alpha|^2 / \bar{n}_{th}$ increases as shown in Fig. S1a. By turning on and off quantum coherence, the ratio can be measured. After the equilibrium time $1/\Gamma_r$, $g^{(2)}(t)$ converges to unity, and therefore

$$g^{(2)}(t) = 1 + \frac{1 + 2|\alpha|^2 / \bar{n}_{th}}{(1 + |\alpha|^2 / \bar{n}_{th})^2} e^{-|\Gamma_r t|}. \tag{S21}$$

The analytic solution Eq. (S21) and the experimental result in Fig. S1b show a good agreement.

When the pump and cavity frequencies are the same, all atoms have the same phase, resulting in superradiance. If the detuning between the pump laser and the cavity is much larger than the cavity linewidth, the atoms are no longer superradiant, and thus the cavity field diminishes. It can be confirmed by measuring the photon number in the cavity while scanning the pump laser frequency across the cavity resonance as shown in Fig. S2. The broad Gaussian envelope centered at the atomic transition frequency has the width determined by the transit time of the atoms across the pump laser beam and the cavity. A Lorentzian sharp peak centered at each cavity frequency under the envelope is the superradiant signal. As the cavity frequency varies, the location of the sharp peak shifts along.

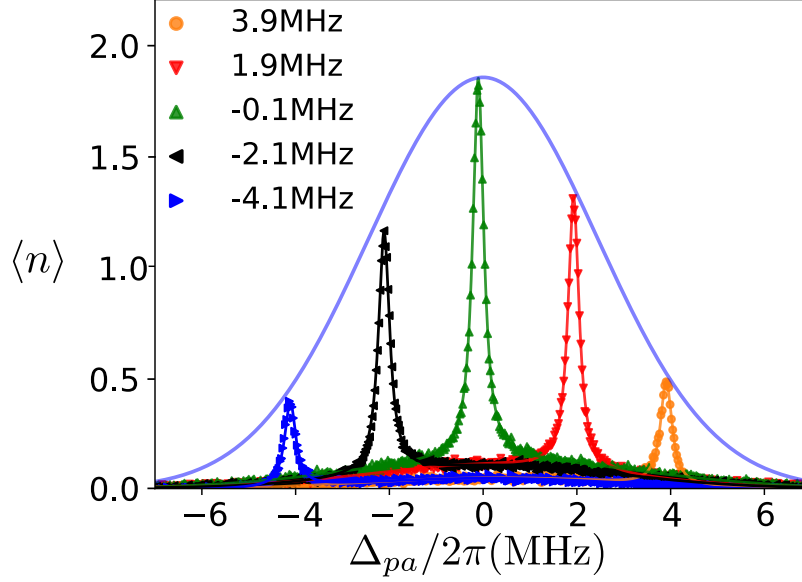


FIG. S2. **Pump-atom detuning dependence of the superradiance signal for various cavity-atom detuning.** Symbols represent experimental data and lines are Lorentz fits. The solid light-blue line is a theoretical envelope determined by the transit time broadening.

3. ENTROPY OF THE ENGINE

According to Ref. [4], the density operator of the thermal coherent state can be written as

$$\rho = D(\alpha)\rho_{\text{th}}D^\dagger(\alpha) = \frac{1}{\bar{n}_{\text{th}} + 1} \left(\frac{\bar{n}_{\text{th}} + 1}{\bar{n}_{\text{th}}} \right)^{-(\alpha^\dagger - \alpha^*)(a - \alpha)}. \quad (\text{S22})$$

With the logarithm of the operator $\log \rho = -\log(\bar{n}_{\text{th}} + 1) - \log\left(\frac{\bar{n}_{\text{th}} + 1}{\bar{n}_{\text{th}}}\right) (a^\dagger - \alpha^*)(a - \alpha)$, the von Neumann entropy for the cavity field can be calculated as

$$\begin{aligned} S/k_B &= -\text{Tr}[\rho \log \rho] \\ &= \log(\bar{n}_{\text{th}} + 1) + \text{Tr} \left[D(\alpha)\rho_{\text{th}}D^\dagger(\alpha) \log \left(\frac{\bar{n}_{\text{th}} + 1}{\bar{n}_{\text{th}}} \right) (a^\dagger - \alpha^*)(a - \alpha) \right] \\ &= \log(\bar{n}_{\text{th}} + 1) + \int \frac{d^2\beta}{\pi} \langle \beta | D(\alpha)\rho_{\text{th}}D^\dagger(\alpha) \log \left(\frac{\bar{n}_{\text{th}} + 1}{\bar{n}_{\text{th}}} \right) (a^\dagger - \alpha^*)(a - \alpha) | \beta \rangle \\ &= \log(\bar{n}_{\text{th}} + 1) \\ &\quad + \int \frac{d^2\beta}{\pi} \langle \beta | D(\alpha)\rho_{\text{th}} \log \left(\frac{\bar{n}_{\text{th}} + 1}{\bar{n}_{\text{th}}} \right) D^\dagger(\alpha) (a^\dagger - \alpha^*) D(\alpha) \\ &\quad \quad \quad D^\dagger(\alpha) (a - \alpha) D(\alpha) D^\dagger(\alpha) | \beta \rangle. \end{aligned} \quad (\text{S23})$$

Using the relations $D(\alpha)^\dagger a D(\alpha) = a + \alpha$, $D(\alpha)^\dagger a^\dagger D(\alpha) = a^\dagger + \alpha^*$, and $D(\alpha)D(\beta) = \exp[i\text{Im}(\alpha\beta^*)]D(\alpha + \beta)$, we find

$$\begin{aligned} S/k_B &= \log(\bar{n}_{\text{th}} + 1) + \int \frac{d^2\beta}{\pi} \langle \beta - \alpha | \rho_{\text{th}} \log \left(\frac{\bar{n}_{\text{th}} + 1}{\bar{n}_{\text{th}}} \right) a^\dagger a | \beta - \alpha \rangle \\ &= \log(\bar{n}_{\text{th}} + 1) + \log \left(\frac{\bar{n}_{\text{th}} + 1}{\bar{n}_{\text{th}}} \right) \text{Tr}[\rho_{\text{th}} a^\dagger a] \\ &= \log(\bar{n}_{\text{th}} + 1) + \bar{n}_{\text{th}} \log \left(\frac{\bar{n}_{\text{th}} + 1}{\bar{n}_{\text{th}}} \right) = (\bar{n}_{\text{th}} + 1) \log(\bar{n}_{\text{th}} + 1) - \bar{n}_{\text{th}} \log(\bar{n}_{\text{th}}). \end{aligned} \quad (\text{S24})$$

The entropy is independent of α , thus the entropy of the thermal coherent state is the same as that of the thermal state.

During the isochoric process, the field state changes from the thermal state to the thermal coherent state, vice versa, for the same reservoir temperature. Consequently, the entropy of the engine or the cavity field does not change. However, we have shown in Methods that heat Q_{ab} is absorbed by the engine from the reservoir during the isochoric process $a \rightarrow b$. Heat transfer without a change in the engine entropy may appear to contradict the second law of thermodynamics. We show below that it is not the case.

4. ERGOTROPY TRANSFER FROM THE RESERVOIR

Ergotropy is defined as the maximum extractable work from a non-passive state[5]. It can be evaluated as

$$\mathcal{E} = \sum_{j,l} r_j \varepsilon_l (|\langle r_j | \varepsilon_l \rangle|^2 - \delta_{jl}), \quad (\text{S25})$$

where the state and Hamiltonian is given as

$$\rho \equiv \sum_{j \geq 1} r_j |r_j\rangle \langle r_j|, \quad H \equiv \sum_{l \geq 1} \varepsilon_l |\varepsilon_l\rangle \langle \varepsilon_l|, \quad r_1 \geq r_2 \geq \dots, \quad \varepsilon_1 \leq \varepsilon_2 \leq \dots. \quad (\text{S26})$$

Let us consider the simplified scenario in which atoms initially prepared in the same superposition state $\sqrt{\rho_{gg}} |g\rangle + \sqrt{\rho_{ee}} |e\rangle$ (with $\rho_{gg} > \rho_{ee}$) coherently emit photons to a lossless cavity on resonance. The eigenstates are ground and excited states $|\varepsilon_{1(2)}\rangle = |g(e)\rangle$, and $r_1 = 1$ because the prepared state is a pure state. Then the ergotropy change of the reservoir is equal to the variation of the energy stored in the atoms:

$$\Delta \mathcal{E} = \hbar \omega_a \sum_k \Delta \rho_{ee,k}, \quad (\text{S27})$$

where $\rho_{ee,k}$ represents the excited state population of the k th atom.

Recently, It has been pointed out that the law of thermodynamics should be modified to include coherence in the quantum regime as follows[6]:

$$T_R \Delta S \geq \Delta Q + T_R \Delta \mathcal{C}, \quad (\text{S28})$$

where \mathcal{C} is the relative entropy of coherence of the reservoir as defined as

$$\mathcal{C}/k_B \equiv \text{tr} [\rho_R \log \rho_R - \rho_R^d \log \rho_R^d], \quad (\text{S29})$$

where $\rho_R(\rho_R^d)$ is (the diagonal part of) the density matrix of the reservoir. The relative entropy of coherence for the k th atom can be written as

$$\begin{aligned} \mathcal{C}_k/k_B = & \text{tr} \left[\left(\begin{array}{cc} \frac{\rho_{ee,k}}{\sqrt{\rho_{gg,k} \rho_{ee,k}}} & \frac{\sqrt{\rho_{gg,k} \rho_{ee,k}}}{\rho_{gg,k}} \end{array} \right) \log \left(\begin{array}{cc} \frac{\rho_{ee,k}}{\sqrt{\rho_{gg,k} \rho_{ee,k}}} & \frac{\sqrt{\rho_{gg,k} \rho_{ee,k}}}{\rho_{gg,k}} \end{array} \right) \right] \\ & - \text{tr} \left[\left(\begin{array}{cc} \rho_{ee,k} & 0 \\ 0 & \rho_{gg,k} \end{array} \right) \log \left(\begin{array}{cc} \rho_{ee,k} & 0 \\ 0 & \rho_{gg,k} \end{array} \right) \right]. \end{aligned} \quad (\text{S30})$$

The first term is the entropy of the atom in a pure state, and therefore, it vanishes. Equation (S30) is then reduced to

$$\begin{aligned} \mathcal{C}_k/k_B = & -\rho_{ee,k} \log \rho_{ee,k} - \rho_{gg,k} \log \rho_{gg,k} \\ = & -\rho_{ee,k} \log \rho_{ee,k} - (1 - \rho_{ee,k}) \log(1 - \rho_{ee,k}). \end{aligned} \quad (\text{S31})$$

When the change in the atomic state while traversing the cavity is small, the change in the relative entropy can be approximated as

$$\begin{aligned} \Delta \mathcal{C}_k/k_B = & (-1 - \log \rho_{ee,k}) \Delta \rho_{ee,k} + [1 + \log(1 - \rho_{ee,k})] \Delta \rho_{ee,k} \\ = & \log(\rho_{gg,k}/\rho_{ee,k}) \Delta \rho_{ee,k} \simeq \log(\rho_{gg}/\rho_{ee}) \Delta \rho_{ee,k}. \end{aligned} \quad (\text{S32})$$

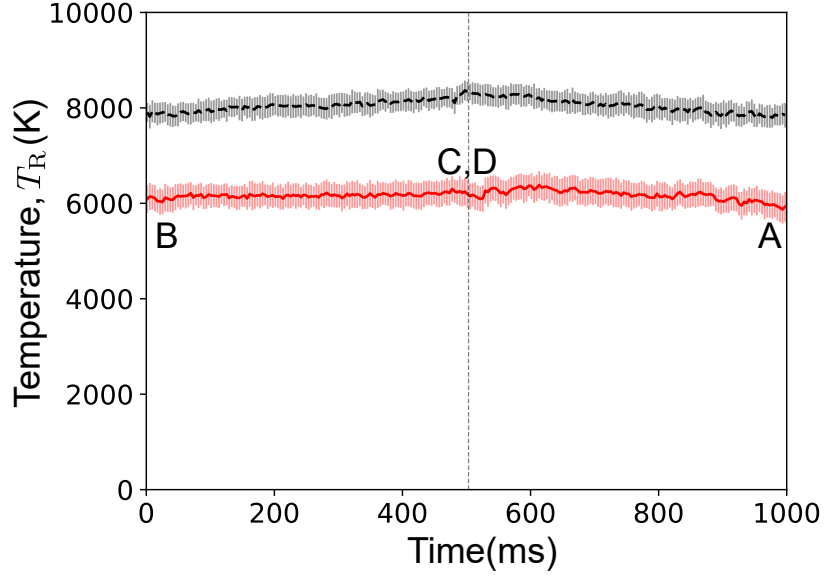


FIG. S3. **Effective temperature of the reservoir controlled during the cycle.** The average temperature of black dashed and red solid lines are 8000K and 6200K, respectively. Data are presented as mean values and error bars shown as shaded vertical lines are one standard deviations from 60 repeated measurements.

For the isochoric process $A \rightarrow B$, $\Delta S = 0$ and thus Eq. (S28) then becomes

$$\begin{aligned} \Delta Q &\leq -T_R \Delta \mathcal{E} = -\frac{\hbar \omega_a}{k_B \log(\rho_{gg}/\rho_{ee})} \sum_k \Delta \mathcal{E}_k \\ &= -\hbar \omega_a \sum_k \Delta \rho_{ee,k} = \hbar \omega_a \Delta n \end{aligned} \quad (\text{S33})$$

where we used the definition of the reservoir temperature, Eq. (9), with $\kappa = 0$ and the energy conservation $\Delta n + \sum_k \Delta \rho_{ee,k} = 0$ for the lossless cavity, for which the equality holds. Equation (S33) shows that the heat absorbed by the engine in the isochoric process indeed comes from the change in the relative entropy of coherence for the reservoir. Note that the negative of the ergotropy change, $-\Delta \mathcal{E}$, of the superradiant reservoir in Eq. (S27) is equal to the energy transfer, $\Delta Q = -T_R \Delta \mathcal{E}$, that occurs when the relative entropy of coherence changes. The relationship between the two concepts has been revealed for more general cases[7].

5. ENGINE CONTROL

During the isoenergetic processes ($B \rightarrow C$ and $D \rightarrow A$), the internal energy of the working fluid ($n\hbar\omega_c$) is kept constant. In the case of our engine, the photon number is almost constant in the expansion and compression stage because the change in ω_c is in the order of 10^{-9} with respect to its mean value. However, the gain profile of the atoms depends on the atom-cavity detuning, so the temperature of the reservoir should be adjusted in order to keep the photon number constant as shown in Fig. S3. Experimentally, the power of the pump laser is manipulated. To estimate the effective temperature of the reservoir, we employ the $^1S_0 \leftrightarrow ^1P_1$ cycling transition (553 nm). By comparing the fluorescence of the 553-nm cycling transition when the 791-nm pump is turned on and off, the excited state population can be inferred (*i.e.* shelving experiment). The effective reservoir temperature is then obtained from Eq. (9). As the mean temperature decreases, the necessary change in temperature to maintain the internal energy becomes negligible (red line in Fig. S3).

Our engine is not autonomous. That is, the mirrors are not pushed or pulled by radiation pressure alone, but the distance between two mirrors or the resonance frequency of the cavity is modulated externally, as in other quantum engine experiments[8–10]. We measured the resonance frequency of the cavity, which can be converted to the distance between the mirror, from the cavity transmission spectrum. For the data shown in Fig. 1d, the cavity frequency change is inversely proportional to the cavity length change and the 0.5 MHz scan range corresponds to a length change of 1.3×10^{-12} m, about 1/40 of the Bohr radius. Such a small change can be controlled by using a feedback

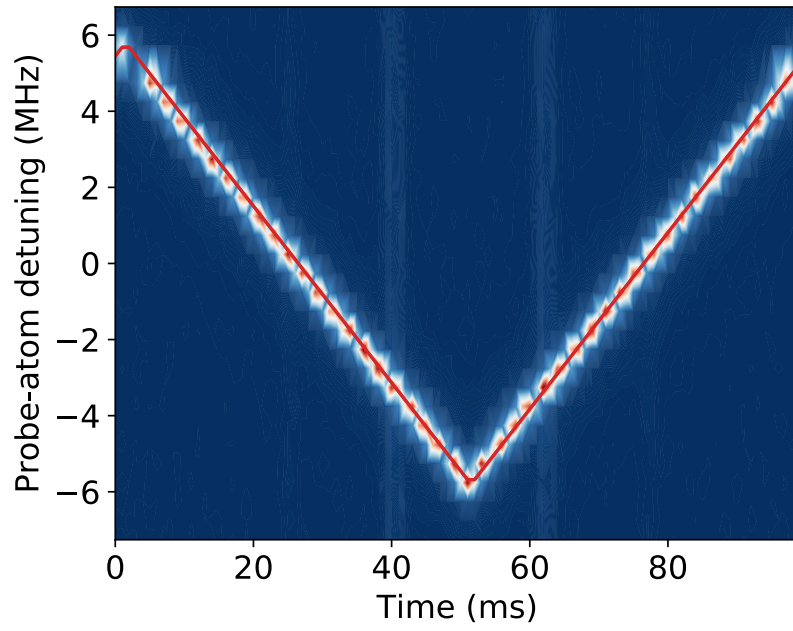


FIG. S4. **Cavity frequency control** Cavity output field detected by a single photon counting module. The red line is the expected cavity frequency.

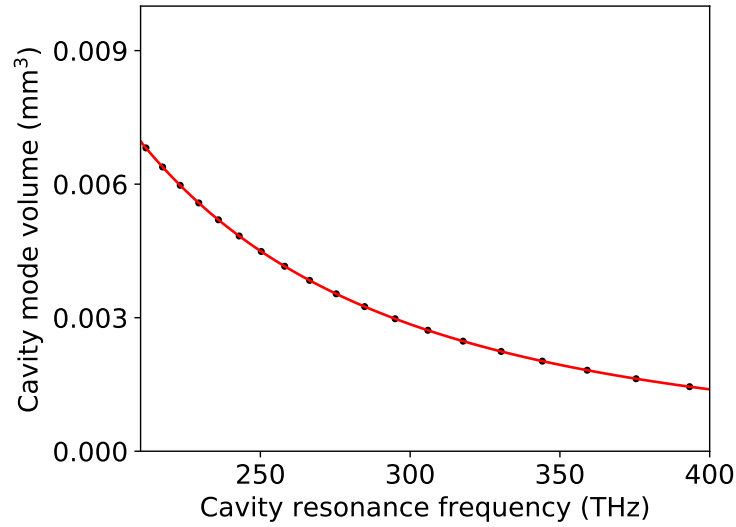


FIG. S5. **The cavity resonance frequency dependence of the cavity mode volume.** Black circles correspond the numerically calculated result and red solid curve is the analytic solution.

loop. By manipulating the applied voltage to the piezoelectric transducer, the resonance frequency of the cavity can be adjusted. From the measured transmission spectrum of the cavity, the resonance frequency can be deduced as shown in Fig. S4.

6. RELATIONSHIP BETWEEN VOLUME(PRESSURE) AND CAVITY RESONANCE FREQUENCY(PHOTON NUMBER)

The x axis of the pressure-volume diagram in Fig. 1d in the main text is represented by the cavity resonance frequency, and the y axis is represented by the number of photons. Here is the explicit relations between pressure(volume) and photon number(cavity resonance frequency).

The cavity mode used in experiments is the TEM00 Gaussian mode with l anti-nodes along the cavity axis which can be expressed as[11]

$$E(x, y, z) = \frac{w_m}{w(x)} e^{-\frac{r^2}{w^2(x)}} \cos \left[k_l x - \arctan \left(\frac{x}{x_0} \right) + \frac{k_l r^2}{R(x)} + (l-1) \frac{\pi}{2} \right], \quad (\text{S34})$$

where w_m is the cavity waist, k_l is the wave number, x_0 is the Rayleigh range, $r \equiv \sqrt{y^2 + z^2}$, and the spot size parameter $w(x)$ and the curvature at position x , $R(x)$ are given by

$$w(x) = w_m \sqrt{1 + (x/x_0)^2}, \quad (\text{S35})$$

$$R(x) = x \left[1 + (x_0/x)^2 \right]. \quad (\text{S36})$$

Then, the resonance frequency of the modes are

$$\nu_l = \left[l + \frac{2}{\pi} \arctan \left(\frac{L}{2x_0} \right) \right] \nu_F, \quad (\text{S37})$$

with the distance between the mirrors L , and the free spectral range $\nu_F = \frac{c}{2L}$. Because $L(1.1 \text{ mm}) \ll x_0(7.4 \text{ mm})$, the following approximations are valid: $w_m \simeq w(x)$, and $\arctan \left(\frac{x}{x_0} \right) \ll 1$. Then, the cavity mode and its resonance frequency can be approximated as

$$E(x, y, z) \simeq e^{-\frac{r^2}{w_m^2}} \cos \left[k_l x + (l-1) \frac{\pi}{2} \right], \quad (\text{S38})$$

$$\nu_l \simeq \frac{lc}{2L}. \quad (\text{S39})$$

Therefore, the mode volume of the Fabry-Pérot cavity can be written as

$$V_m = \int_{-L/2}^{L/2} dx \int_0^{2\pi} d\theta \int_0^\infty dr |E(r, \theta, x)|^2 \simeq \frac{1}{4} \pi w_m^2 L = \frac{\pi \sqrt{2R}}{4k_l} L^{3/2} = \frac{\pi \sqrt{Rl^3 c^3}}{8k_l} \nu_l^{-3/2}, \quad (\text{S40})$$

where θ is the polar angle. The analytic solution Eq. (S40) and the mode volume obtained by numerically integrating Eq. (S34) are compared in Fig. S5.

The radiation pressure is represented by the photon number. Let us consider a cylinder consisting of perfect mirrors($L \times A$ (area)). The round trip time between the two mirrors is $2L/c$, and the amount of momentum transferred in one collision is $2\hbar k_l$. Therefore pressure on the wall is given by

$$P = \frac{2n\hbar k_l/A}{2L/c} = \frac{n\hbar\omega_c}{AL} = \frac{n\hbar\omega_c}{V_m}, \quad (\text{S41})$$

where n is the number of photons bouncing along the cavity axis.

* kwan@phya.snu.ac.kr

[1] Stenholm, S. Quantum theory of electromagnetic fields interacting with atoms and molecules. *Phys. Rep.* **6**, 1–121 (1973).
 [2] Yang, D. *et al.* Realization of superabsorption by time reversal of superradiance. *Nat. Photonics* **15**, 272–276 (2021).

- [3] Scully, M. O. & Zubairy, M. S. *Quantum optics* (1999).
- [4] Vogel, W. & Welsch, D.-G. *Quantum optics* (John Wiley & Sons, 2006).
- [5] Allahverdyan, A. E., Balian, R. & Nieuwenhuizen, T. M. Maximal work extraction from finite quantum systems. *Europhys. Lett.* **67**, 565 (2004).
- [6] Ma, Y.-H., Liu, C. & Sun, C. Works with quantum resource of coherence. *arXiv preprint arXiv:2110.04550* (2021).
- [7] Francica, G. *et al.* Quantum coherence and ergotropy. *Phys. Rev. Lett.* **125**, 180603 (2020).
- [8] Klaers, J., Faelt, S., Imamoglu, A. & Togan, E. Squeezed thermal reservoirs as a resource for a nanomechanical engine beyond the carnot limit. *Phys. Rev. X* **7**, 031044 (2017).
- [9] Klatzow, J. *et al.* Experimental demonstration of quantum effects in the operation of microscopic heat engines. *Phys. Rev. Lett.* **122**, 110601 (2019).
- [10] Bouton, Q. *et al.* A quantum heat engine driven by atomic collisions. *Nat. Commun.* **12**, 1–7 (2021).
- [11] Haroche, S. & Raimond, J.-M. *Exploring the quantum: atoms, cavities, and photons* (Oxford university press, 2006).